Langmuir

Article

pubs.acs.org/Langmuir

Humidified Microcontact Printing of Proteins: Universal Patterning of Proteins on Both Low and High Energy Surfaces

Sébastien G. Ricoult,[†,‡,§] Amir Sanati Nezhad,[†,‡] Michaela Knapp-Mohammady,[∥] Timothy E. Kennedy,[§] and David Juncker*[,†,‡,§]

[†]Department of Biomedical Engineering, McGill University, Montreal, Quebec H3A 2B4, Canada

[‡]McGill University & Genome Quebec Innovation Centre, McGill University, Montreal, Quebec H3A 0G1, Canada

[§]McGill Program in Neuroengineering, Department of Neurology and Neurosurgery, Montreal Neurological Institute, McGill University, Montreal, Quebec H3A 2B4, Canada

[∥]Division of Functional Genome Analysis, German Cancer Research Center (DKFZ), Im Neuenheimer Feld 580, Heidelberg 69120, Germany

Supporting Information

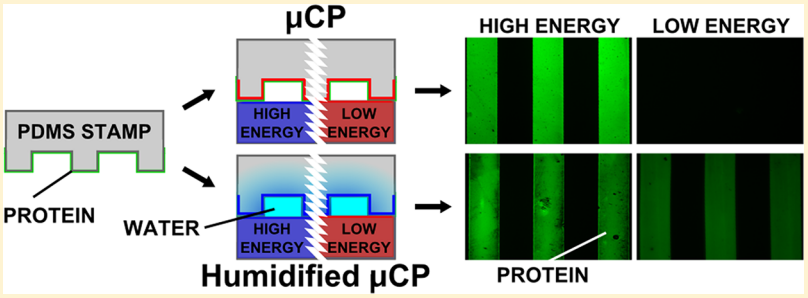

ABSTRACT: Microcontact printing (μCP) of proteins is widely used for biosensors and cell biology but is constrained to printing proteins adsorbed to a low free energy, hydrophobic surface to a high free energy, hydrophilic surface. This strongly limits μCP as harsh chemical treatments are required to form a high energy surface. Here, we introduce humidified μCP (HμCP) of proteins which enables universal printing of protein on any smooth surface. We found that by flowing water in proximity to proteins adsorbed on a hydrophilized stamp, the water vapor diffusing through the stamp enables the printing of proteins on both low and high energy surfaces. Indeed, when proteins are printed using stamps with increasing spacing between water-filled microchannels, only proteins adjacent to the channels are transferred. The vapor transport through the stamp was modeled, and by comparing the humidity profiles with the protein patterns, 88% relative humidity in the stamp was identified as the threshold for HμCP. The molecular forces occurring between PDMS, peptides, and glass during printing were modeled *ab initio* to confirm the critical role water plays in the transfer. Using HμCP, we introduce straightforward protocols to pattern multiple proteins side-by-side down to nanometer resolution without the need for expensive mask aligners, but instead exploiting self-alignment effects derived from the stamp geometry. Finally, we introduce vascularized HμCP stamps with embedded microchannels that allow printing proteins as arbitrary, large areas patterns with nanometer resolution. This work introduces the general concept of water-assisted μCP and opens new possibilities for "solvent-assisted" printing of proteins and of other nanoparticles.

INTRODUCTION

Surface patterning of proteins at micrometer resolution is of interest to replicate simplified patterns from the *in vivo* environment *in vitro* to study complex cellular mechanisms such as adhesion,[1,2] migration,[3] or apoptosis.[4] Microcontact printing (μCP) of proteins using elastomeric poly-(dimethylsiloxane) (PDMS) stamps was first reported in 1998.[5] The process of μCP of proteins involves first adsorbing proteins onto a PDMS stamp, briefly drying the stamp under a stream of nitrogen, and then gently transferring the proteins onto a plasma activated glass surface, without need for chemical cross-linking at the surface. A particularity of μCP of proteins is the absence of a viscous, liquid ink during the printing and the lack of protein diffusion following adsorption. Instead, conventional printing involves the transfer of a viscous ink or, in the case of μCP of thiols or silanes, of molecules that are dissolved in the stamp and diffuse in and across the stamp as well as across the gaps during printing. In contrast, proteins behave as globular particles that are immobilized following adsorption on the stamp surface and that are transferred with exquisite accuracy without blurring by diffusion and reaching single molecule resolution.[6] μCP of proteins requires (i) "inking" of the stamp with a protein that spontaneously adsorb on a low free energy, hydrophobic surface, often PDMS, and

Received: July 11, 2014
Revised: September 3, 2014
Published: September 15, 2014

(ii) printing onto a high energy, hydrophilic surface which upon separation of the stamp results in the transfer of the protein to the target surface. The physicochemical phenomena governing the transfer from stamp-to-surface are not fully understood, but it was found empirically that μCP of proteins must proceed from a low energy stamp to a high energy surface, which was experimentally confirmed using various stamp materials and surfaces.[7] Chen and colleagues characterized printing as a function of surface energy and found that as the free energy of the surface decreases, transfer efficacy diminishes and fails completely on low energy, hydrophobic surfaces.[8] Thus, μCP of proteins operates under the paradigm from low to high energy surface, which simultaneously constitutes one of the greatest limitations as μCP of proteins is restricted to high energy surfaces only. In a standard laboratory environment, the normal, stable state of a surface is low energy. Harsh chemical treatments, for example using a plasma,[9] are needed to create reactive, high energy surfaces and are widely used with glass, or silicon oxide,[10] as well as with some polymers.[11] However, a high energy state is unfavorable, and surfaces spontaneously revert to a low energy state either by chemical reaction of the activated groups, by adsorption of contaminants from the environment[12] or, as in the case of PDMS, by diffusion of nonpolymerized monomers from within the material.[13] As proteins and other biomolecules cannot withstand the harsh treatments required for surface activation, the printing process has to be completed rapidly after activation, and no further treatments are possible thereafter, thus limiting the possibility to pattern multiple proteins on a surface. It is possible to print on hydrophobic surfaces using other soft lithography methods, for example hydrogel-based stamping.[14] However, in contrast to μCP, the proteins remain dissolved within the soft hydrogel and freely diffuse. Furthermore, the stamps were found to slide on the surface, thus limiting resolution to 50 μm and introducing variability in print quality and feature size.

One further limitation of conventional microcontact printing is the restriction of a single ink per stamp. In order to overcome this limitation, microfluidics has been used to pattern different concentrations of a same protein in adjacent channels.[15] Microfluidics has also been combined with microcontact printing to flow solutions in the capillaries formed by the stamp contacting the surface[16,17] or by printing linkers in the microfluidic device to then capture flown molecules.[17,18] Alternatively, heat induced swelling of a nanoparticle doped polymer stamp creates infoldings which protect areas from protein adsorption and facilitate the binding of multiple proteins.[19] Even though efficient, the implementation of microfluidics or heat activated stamps in the printing process is limited by geometry where continuous channels are required for microfluidics or infoldings for heat activated stamps. Lift-off or stamp-off techniques have also been used to remove specific portions of the pattern and backfill the gaps with other biomolecules.[20,21] This approach has been shown to work for a number of cases; however, cross-contamination of the first stripe remains a concern that may occur for (i) molecules that have an affinity for one another, (ii) in cases where the second molecule can adsorb onto unoccupied spaces between the first molecule, or (iii) if it desorbs and replaces the first molecule during the bulk incubation. Complex alignment techniques have also been developed to align multiple stamps onto a same substrate; however, alignment remains challenging and slow and requires specialized equipment.[22,23]

Here we introduce humidified microcontact printing (HμCP) which can transfer proteins adsorbed onto a stamp to both low energy and high energy surfaces. HμCP is based on (i) a hydrophilic PDMS stamp and (ii) humidification of the interface by diffusion from a water reservoir to effect the transfer of proteins. HμCP is illustrated by printing proteins on a variety of surfaces. Molecular models of the interaction of a peptide sandwiched between PDMS and SiO_2 (glass) confirm the intercalation of H_2O molecules between protein and high energy surfaces. The role of humidification is characterized and validated using a combination of modeling and experiments based on stamps with channels with increasing separation. The potential of HμCP is illustrated by multiprotein prints in combination with μCP facilitating the printing of proteins side-by-side and on top of one another. Finally, following a better understanding of the parameters governing the protein transfer, we designed vascularized stamps with embedded channels that allow arbitrary patterns to be transferred, with feature sizes ranging from millimeters to nanometers.

RESULTS AND DISCUSSION

Whereas it was not believed possible to print proteins from a high energy to a low energy surface, we discovered that by filling water into microchannels structured as bas relief into the surface of the stamp, proteins in proximity of the channels could be transferred onto a low energy surface. PDMS is permeable to water vapor,[24] and hence water molecules diffuse through the PDMS to the (high energy) surface of the stamp at the interface with the substrate and thereby humidify the proteins. To highlight the similarities and differences of μCP and HμCP, flowcharts for both processes are shown in Figure 1a,b. For HμCP, the proteins are first adsorbed from solution on a flat, low energy stamp, which is used for "dry inking" (not shown here) of a plasma activated, high energy stamp structured with microchannels by printing on it, and thus transferring the proteins. The inked stamp (first schematic in Figure 1b) is then used for HμCP by printing it onto any desired low energy surface in a dry state, followed by flowing water through the microfluidic channels. Figure 1c shows a surface patterned with a stamp featuring 10×10 μm^2 wide ridges separated by 100 μm wide channels. Only the channels on the right half of the stamp were filled with water, which (i) illustrates the requirement for water to transfer the proteins and (ii) indicates that the diffusion length is limited.

To demonstrate the versatility and strength of HμCP, it was used to print various proteins on hydrophobic surfaces and the results compared to the ones obtained by conventional μCP. The ability of HμCP to transfer proteins on conventionally unprintable surfaces was first demonstrated by adding water to a stamp in contact with a surface that could otherwise not be patterned prior to the addition of water. Within a minute of the addition of water, protein could now be transferred to the hydrophobic surface (Figure S1). To evaluate whether HμCP was applicable to various proteins, bovine serum albumin and the peptide arginine-glycine-aspartic acid (RGD) were printed onto the PDMS surface. The transfer was excellent for both proteins (Figure S2), suggesting that HμCP is generally applicable to proteins and peptides.

To characterize transfer as a function of the surface energy, both μCP and HμCP were used to print onto eight flat substrates, including plasma or nitric acid cleaned glass, epoxysilane-, aldehydesilane-, aminosilane-, or fluorosilane-coated glass as well as polystyrene and PDMS (Figure 2).

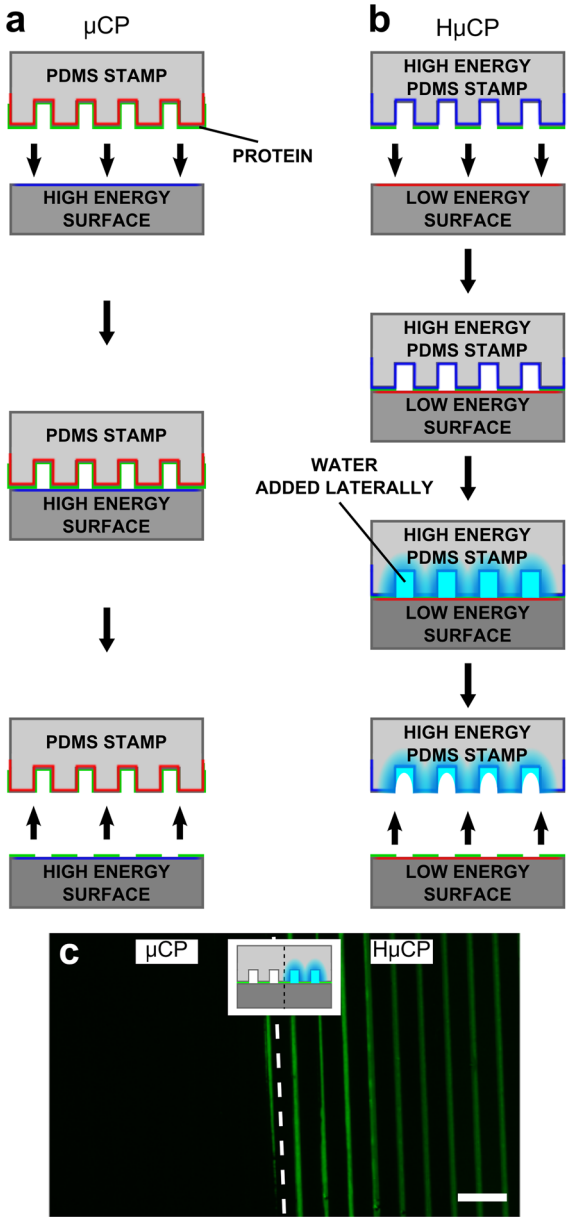

Figure 1. μCP and humidified μCP of proteins. Process flow comparisons of (a) direct μCP and (b) HμCP of proteins. In standard μCP, a low energy stamp (red) is used to transfer protein by printing onto a higher energy surface (blue). In contrast, HμCP employs high energy stamps and can transfer protein onto low energy surfaces by adding water. Plasma activated structured stamps patterned with protein are contacted with low energy surfaces in a dry state. A solution is flowed through the capillaries of the stamp by filling the channels from the edge and then incubating the solution for five min before separating the stamp from the surface. High energy surfaces are highlighted in blue and low energy surfaces in red. (c) HμCP of fluorescently labeled IgG printed onto a nonactivated glass substrate. Only the right half of the channels were filled with water, but not the left half, which led to transfer on only half of the surface coinciding with the location of the filled channels. The scale bar is 250 μm.

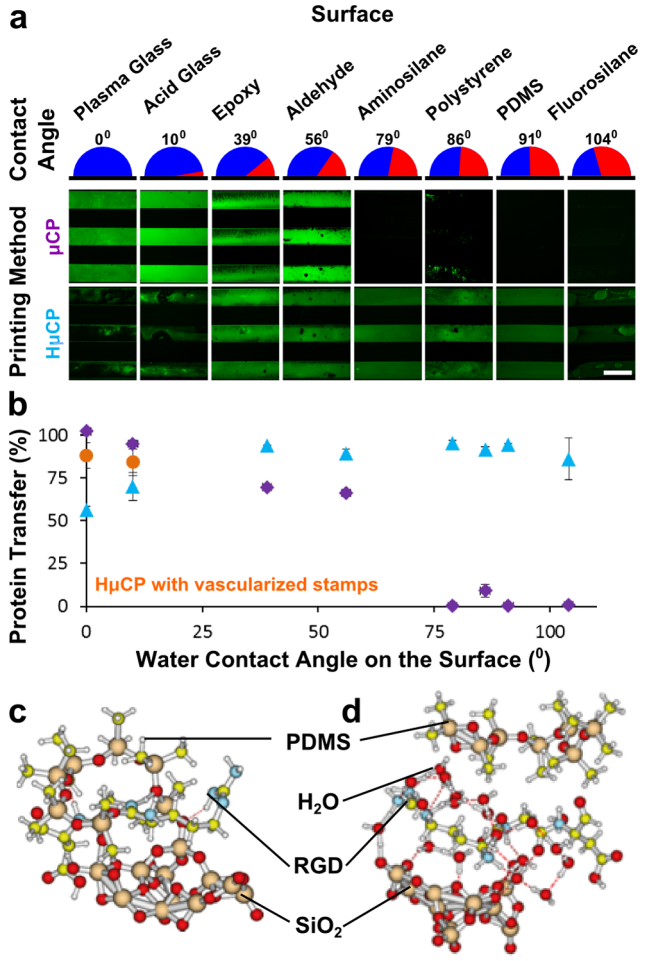

Figure 2. Patterning of proteins on different surfaces with varying wettability by μCP and HμCP and models of RGD adhesion in dry and wet state between SiO_2 and PDMS. (a) The contact angle for each surface was measured and is indicated on top. Representative images of fluorescently labeled IgG printed by conventional μCP and by HμCP. The target surfaces were glass slides cleaned with plasma or nitric acid or coated with epoxy, aldehyde, aminosilane, or fluorosilane as well as polystyrene and PDMS. (b) Data from (a) were quantified to assess protein transfer achieved through μCP (purple) and HμCP (blue) based on the percentage of the printed area that has been coated with protein. Quantification of HμCP with vascularized stamps on the most wetting surfaces is also represented on the dot plot (orange). Percentage protein transfer has been plotted with respect to the surface wettability. Error bars are standard deviation, n = 3–9. Scale bar is 200 μm. *Ab initio* model of the RGD peptide sandwiched between a string of SiO_2 and PDMS (c) without and (d) with water. Models are composed of carbon (yellow), hydrogen (white), nitrogen (blue), and oxygen (red) atoms and silicium (pink) and were visualized with the Molden program.

The surface energy was assessed by measuring the contact angle of water, which ranged from 0° for plasma activated glass to 104° for fluorosilane-coated glass. μCP produces spotless patterns on plasma and acid cleaned glass and is effective on epoxy and aldehyde surfaces, but no transfer on aminosilane, PDMS, polystyrene, and fluorosilanes occurred, as expected. Transfer of proteins printed by HμCP was observed on all surfaces, while the best prints were obtained on aminosilane–glass and PDMS. The defects observed on some of the surfaces might not be due to HμCP, but possibly to microscale heterogeneity or dust specks. Although clearly visible, the transfer was weaker and less homogeneous on the fluorosilane and the activated glass surfaces. This result is consistent with the well-known nonstick property of fluoropolymers. Furthermore, the defects observed in the highly hydrophilic surfaces (i.e., plasma and acid cleaned glass) result from water leakage which breaks the conformal contact between the stamp

dx.doi.org/10.1021/la502742r | *Langmuir* 2014, 30, 12002–12010

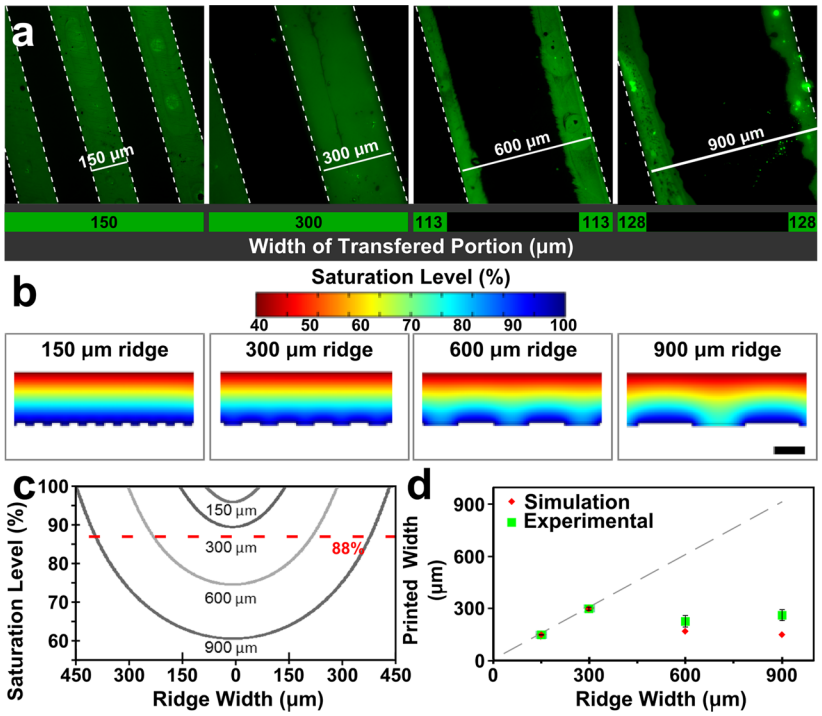

Figure 3. Relationship between protein transfer, ridge width, and water saturation. Representative images of HμCP of fluorescent IgGs with stamps with ridges of (a) 150, 300, 600, and 900 μm widths. The width of protein transferred by each print is indicated below the images. The transfer of IgGs is complete for stripes narrower than 300 μm in width, but partial for wider ridges. (b) Finite element models of water saturation across the different ridges in a. The scale bar is 500 μm. (c) Shows the water saturation level across ridges 150−900 μm in width. A relative water saturation of 88% was identified as the threshold between no transfer and transfer of proteins (dashed red line). (d) Simulation and experimental results (mean ± SD, n = 5−12) of ridge width versus printed width showing good agreement with the 88% humidity threshold value.

and the surface, required for the transfer of protein. Avoiding the delivery of water to the surface can overcome this problem as will be discussed further below.

To gain insight into the adhesion of proteins to PDMS and SiO_2, we performed *ab initio* molecular simulations of a sandwiched RGD peptide between low energy PDMS and high energy SiO_2. RGD can be printed like a regular protein, and although the geometry of the model differs from the experimental setup, the chemical nature of the interactions is captured in the model. In the simulation, both RGD and PDMS adopt a linear conformation while SiO_2 molecules form a rigid scaffold. The results of the quantum mechanical simulation of RGD sandwiched between SiO_2 and PDMS without (Figure 2c) and with water (Figure 2d) are shown. In the absence of water, a close interaction occurs between RGD and both PDMS and SiO_2. When H_2O molecules are included, they surround the RGD and form a layer between the peptide and SiO_2, forming multiple hydrogen bonds, but they do not intercalate significantly between RGD. The methyl groups of PDMS rotate around the backbone and shield the Si−O groups, and no direct hydrogen bonds are formed between PDMS and water molecules. Yet in the absence of water, the RGD peptide conforms to the PDMS. This result is consistent with the transfer of proteins from PDMS to SiO_2 in the dry state, while under humidified conditions water molecules are trapped between the RGD and SiO_2 and prevent the adhesion of the peptide to the SiO_2 or, in the case of HμCP, to the activated, high energy PDMS stamp. A more detailed analysis imposing a planar geometry for SiO_2 and PDMS as well as molecular models that reproduce the elasticity of PDMS will be required to establish a more accurate free energy budget of the different configurations occurring during adsorption, printing, and separation.

Water diffuses laterally from the microchannels into the PDMS, in a gas phase, and the saturation of water is expected to diminish far away from the channels. The transfer of proteins was tested for stamps with 50 μm wide and deep water-filled channels that were separated by ridges with increasing width from 150 to 900 μm. The transfer of proteins was complete close to the microchannels, and on the entire ridge up to 300 μm, but not for wider ridges, where the central part was not transferred (Figure 3a).

To understand the interplay between the diffusion of water and protein transfer, a 2D finite element modelisation (fem) of the relative water saturation at steady state within stamps with different geometries was performed (Figure 3b). The boundaries of the ridges were considered saturated with water and the surfaces in contact with air void of water. By comparing the simulated water saturation profiles (Figure 3c) to the transferred protein patterns, it was found that a threshold of 88% water saturation coincided with the boundary formed between transferred and nontransferred proteins for different designs (Figure 3d).

The diffusion and resulting high saturation of water are key to the transfer of the proteins from the high energy stamp surface to the low energy receiving surface. The concentration of water molecules in PDMS can reach up to 30−40 mol/m^3,[25] which is equivalent to 25−33 L/mol. The concentration of water in air under ambient conditions at saturation is only ∼1 mol/m^3, indicating that PDMS acts as a "sponge" for water vapor. The concentration values in PDMS are consistent with water being in a gaseous phase as they are commensurate with

dx.doi.org/10.1021/la502742r | *Langmuir* 2014, 30, 12002−12010

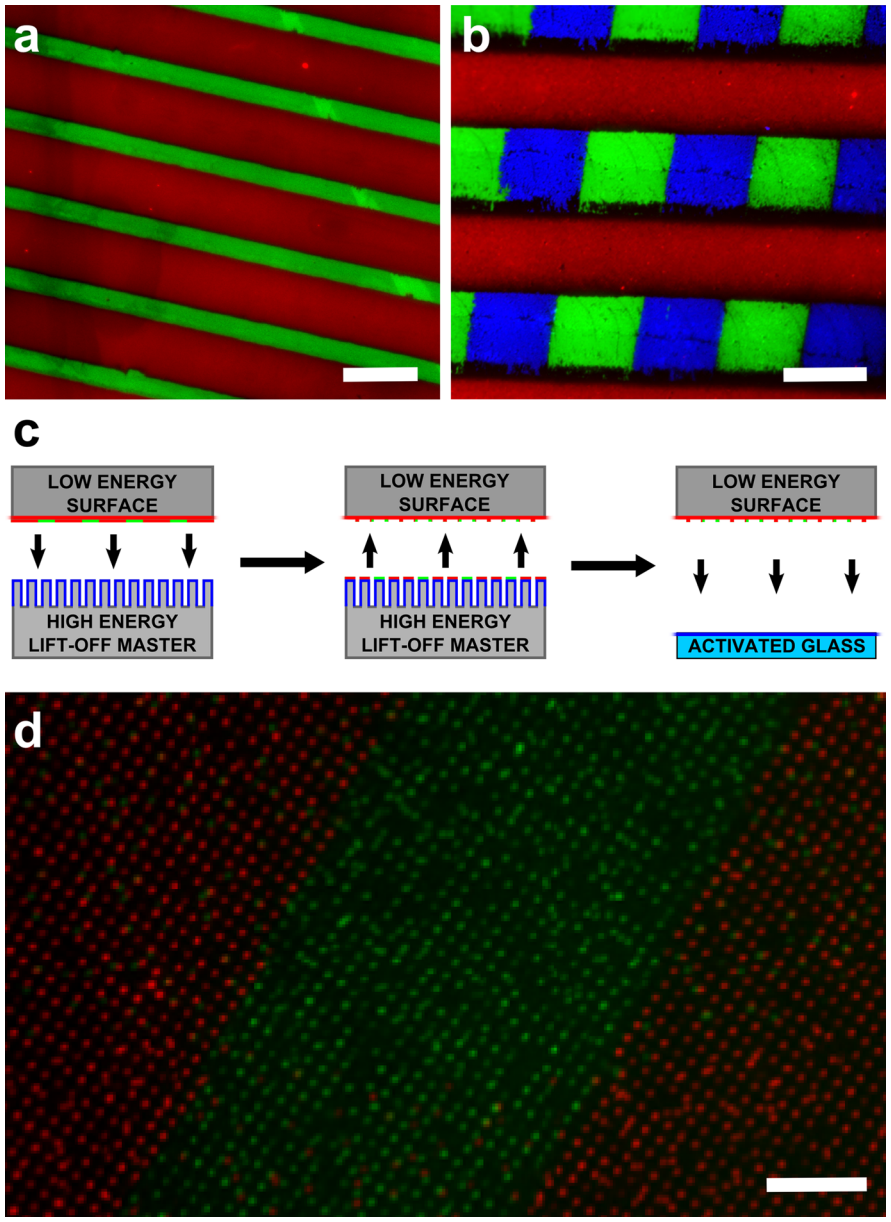

Figure 4. Multiprotein patterning and nanopatterning with HμCP. (a) Green and red fluorescently labeled IgGs were patterned on the same low energy surface using HμCP patterned delivery. (b) Three-protein pattern achieved through HμCP where an array of three labeled IgG's was obtained by repeating HμCP for two consecutive cycles and rotating the flat PDMS stamp 90° after the first round of printing (Figure S5). Black nonpatterned portions visible in the red stripes might be the result of shifting during the last round of "inking" or unsuccessful protein deposition in the microchannels. (c) Schematic of the nanocontact lift-off printing process where the multipatterned stamps are employed further by contacting them with a lift-off master. The lift-off master is then separated from the PDMS stamp, and the remaining nanopatterns at the surface of the PDMS stamp are transferred onto a high energy glass substrate, yielding a multiprotein nanoarray. (d) Fluorescent image of a multiprotein nanoarray composed of 200 nm dots with 1 μm spacing in 20 μm stripes. In this case two IgG's linked to the fluorophores Alexa Fluor 488 and 546 were patterned in juxtaposed nanoarrays. Scale bars are (a) 100, (b) 20, and (d) 10 μm.

the density of an ideal gas in open space (22.4 L/mol).[26] However, the water molecules in the saturated PDMS may condensate at the hydrophilic interface and compete with the proteins for interaction with the stamp surface and at the same time act as a solvent for the proteins. Time course analysis of water saturation at the center of a ridge indicates that the 88% threshold is reached in a few seconds for 150 μm wide ones, while it increases to a few minutes for 300 μm ridges (Figure S3). The presence of water during the printing may thus recreate conditions favorable for the adsorption of proteins to low energy surfaces.

HμCP opens up new possibilities for patterning two and even three different proteins on a surface. Patterning of proteins side-by-side is of interest to many applications such as biosensors and cell navigation and could be done using standard μCP by printing a first one, followed by incubation of the entire surface with a second one. However, this approach suffers from a number of drawbacks. The second protein adsorbed from solution interacts with the immobilized protein initially printed, which may blur the pattern; the target surface has to be of high energy, thus preventing the use of precoated cell culture dishes as well as heterogeneous surfaces such as

dx.doi.org/10.1021/la502742r | *Langmuir* 2014, 30, 12002−12010

biosensors. Proteins in solution do not readily adsorb to high energy surfaces, thus requiring long incubation times while limiting the density of adsorbed protein; finally, it is not possible to pattern a third or any further proteins. With HμCP, two proteins can quickly be patterned side-by-side while avoiding interaction between the two proteins. One protein is patterned by inking the high energy stamp, printing it onto a surface, and the second protein flown through the channels formed between the stamp and the substrate, thus simultaneously adsorbing one protein to the substrate and humidifying the stamp to realize HμCP (Figure 4a). The results show a sharp interface and no overlap of proteins and can easily be used for instance to investigate cell response on multiprotein patterns (Figure S4).

To pattern three proteins side-by-side, stripes of two proteins are first formed on a flat PDMS stamp as described. Next, a plasma activated stamp with embedded channels at a right angle with the protein lines is inked by contacting it with the surface (Figure S5). The inked stamp is then printed onto a low-energy surface while flowing a protein solution through the microchannels and thus transferring all proteins at once (Figure 4b). The two prepatterned proteins form the green and blue arrays, and the flowed protein forms a red stripe. This strategy may be further repeated to pattern more than three proteins by using the three-protein-pattern to ink another structured stamp, and so on, while it is also possible to introduce different patterns.

Nanopatterning with a single kind of protein often uses lift-off printing,[27] but nanopatterns with multiple proteins have been difficult to produce. Using HμCP as described above, different proteins were patterned side-by-side on a flat PDMS stamp, followed by the removal of unwanted areas with a rigid, plasma activated nanostructured master with a negative pattern.[28] Using a PDMS stamp, the residual multiprotein nanopattern was then transferred by μCP on a flat glass surface (Figure 4c,d).

Notwithstanding the above demonstration, the requirement for open channels on the stamp limits the diversity of patterns that can be printed. However, based on the diffusion of water in PDMS, enclosed channels proximal to the stamp surface could create the conditions suitable for HμCP (Figure 5a). A vascularized stamp with channels embedded 100 μm below the surface was made, and the water saturation in PDMS calculated by FEM and found to be adequate for HμCP (Figure 5b,c). Vascularized stamps were created by irreversibly bonding a 100 μm thin PDMS membrane with a structured stamp. Following plasma activation, the vascularized stamp was dry inked by pressing it against a patterned surface coated with proteins and then printed against a target substrate. Water was supplemented with 10% Triton-X 100 (Sigma-Aldrich) to reduce surface tension and filled into the channel by capillary force by adding the water at the open end of the channels, humidifying the stamp and affecting the transfer of proteins. Through the use of vascularized stamps the contact between water and the substrate can be avoided, thus eliminating the creeping of water at the interface between the stamp and surface that interferes with protein transfer and leads to detachment of the stamp from the substrate. With the vascularized stamps, the proteins were transferred with an efficiency rivaling the one achieved by conventional μCP (Figure 2b). The vascularized stamp can also be used for HμCP of large-area protein patterns with nanometer resolution on low energy surfaces (Figure 5d). This print contains a 400 × 400 μm^2 digital nanodot gradient composed of 200 nm dots with decreasing center-to-center

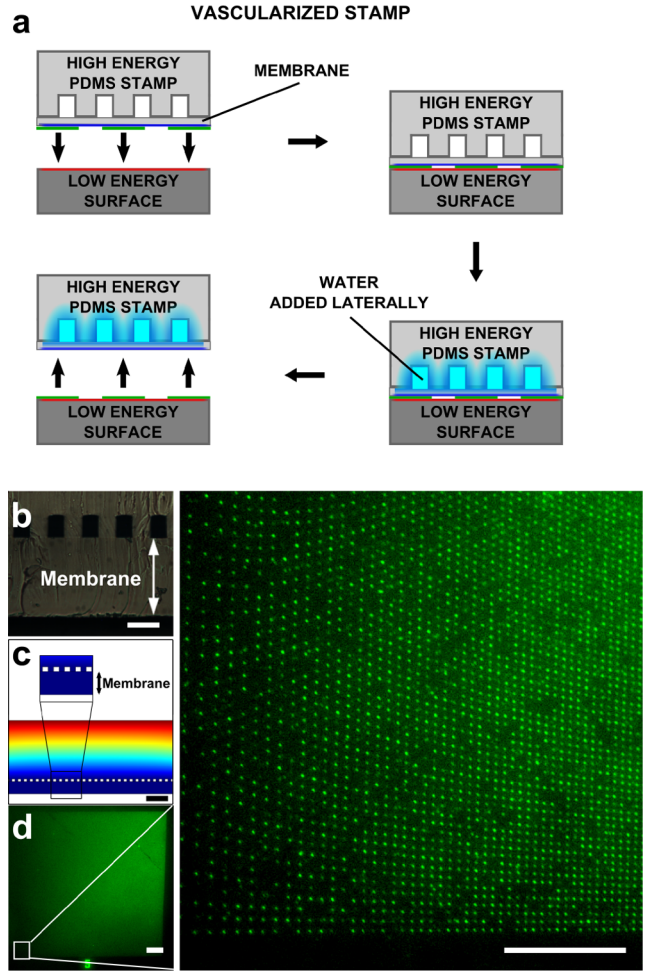

Figure 5. Vascularized stamps allow printing of arbitrary patterns by HμCP down to nanometer resolution. (a) Process flow of HμCP with vascularized stamps. Plasma activated vascularized stamps patterned with protein are contacted with low energy surfaces in a dry state. Next, water with Triton-X100 is flowed through the embedded capillaries of the stamp. After 5 min, the stamp is separated. (b) Cross section of a vascularized stamp and (c) FEM of water saturation within a vascularized stamp. (d) Close-up of a 400 × 400 μm^2 digital nanodot gradient composed of 200 nm wide dots patterned by a vascularized stamp HμCP. The inset shows a close up view revealing individual nanodots. The scale bars are (b) 40, (c) 500, (d) 50 and (inset) 20 μm.

spacing between dots in X and Y from 15 μm to 200 nm over the 400 μm length of the gradient. 400 μm areas could not be printed with the open channel stamps. This demonstration illustrates that large area, high resolution prints can be produced using HμCP.

CONCLUSION

We introduced HμCP for patterning proteins and peptides on any smooth surface regardless of the surface free energy by using hydrophilic, humidified stamps. Using either structured or vascularized stamps with embedded microchannels, multiple proteins were patterned in geometries ranging from millimeter to nanometer resolution. The ability to print on plasma activated glass, which is presumably more hydrophilic than the transfer stamp, underlines that transfer of proteins during HμCP is not dictated by hydrophilicity alone but that other parameters come into play. Thus, further studies, both

dx.doi.org/10.1021/la502742r | Langmuir 2014, 30, 12002−12010

theoretical and experimental, will be needed to uncover the mechanism that enables universal transfer of proteins in HμCP.

Patterning of proteins on low energy surfaces will be of great interest for cell studies that rely widely on low-energy polystyrene substrates for cell culture and for biosensors that encompass a wide range of materials and that often cannot be treated with a plasma chamber. Novel applications can be envisioned, for example, by cyclical picking and printing of proteins in a manner dependent on the affinity of the target surface or of a binding partner coated on the target surface.[17] The addition of solvents other than water might open new avenues for μCP of "bioinks" such as DNA[29] or bacteria[30] as well as for nonbiological materials, including nanowires[31] or graphene,[32,33] on substrates with different surface chemistries and affinities.

METHODS

Experimental Conditions. All experiments were conducted at room temperature and 40−50% humidity.

Surface Preparation. Glass slides (Corning Inc., Corning, NY) were acid cleaned in nitric acid and stored in ethanol. PDMS coated slides were made by coating a thin layer of PDMS on plasma activated glass slides. Epoxy, amminosilane, and aldehyde slides were purchased (Schott, Midland, ON, Canada). Fluorosilane coated slides were made by first plasma activating glass slides and depositing a self-assembled monolayer of perfluorooctyltriethoxysilane (Sigma-Aldrich, Oakville, ON, Canada) in vapor phase in a desiccator for 30 min.

Surface Characterization. The wettability of the different surfaces was assessed by measuring the contact angle of a double distilled water droplet using a contact angle goniometer with video capability (AST, Billerica, MA).

Stamp Preparation. Computer designs of 5 μm in diameter and 5 μm spacing dot arrays, 100 and 10 μm wide stripes with 90 μm spacing were generated in Clewin Pro 4.0 (Wieweb software, Hengelo, Netherlands) and sent out to produce chrome masks (Fineline Imaging, Colorado Springs, CO). Designs of 100, 200, ..., 900, 1000 μm wide stripes with equal spacing were designed in Inkscape and printed on transparencies (MP reproductions, Montreal, QC, Canada). A 4 in. silicon wafer (University Wafers, South Boston, MA) was coated with a layer of SU-8 photoresist (MicroChem, Newton, MA), and the features were patterned through photolithography with a chrome mask or with a transparency. 125 μm diameter spot stamps were obtained as previously reported.[26] Briefly, arrays of circles 125 μm in diameter with a spacing of 150 μm in X and Y direction were designed in Clewin. Upon completion, the files were sent to Lasex (San Jose, CA), where the patterns were laser-etched into 125 μm thick poly(ethylene terephthalate) (PET) with a 501FL 3M adhesive backside. The plastic protective layer was then removed from the sticky side of the PET mask, and the mask was glued onto a clean glass slide. After thorough baking and cleaning, the wafer or PET mask-coated glass slide were coated with an antiadhesive layer by exposing it to perfluorooctyltriethoxysilane (Sigma-Aldrich, Oakville, ON, Canada) in vapor phase in a desiccator. To obtain flat stamps, a native Si wafer was employed. Stamps with the inverse copy of that present on the Si wafer were obtained by pouring 10:1 poly(dimethylsiloxane) (PDMS) on the wafer and curing the polymer for 6 h at 60 °C. The stamps were then cut and cleaned in 70% ethanol for 6 h and baked for 1 h at 60 °C to evaporate all traces of solvent.

Microcontact Printing (μCP). Stamps were ultrasonicated for 5 min in 70% Ethanol prior to the experiment and dried under a stream of N_2. After drying, the patterned stamps were inked with 10 μL of either fluorophore conjugated antibodies (polyclonal, 1:500, Life technologies, Burlington, ON, Canada), fluorescent BSA (Sigma-Aldrich, Oakville, ON, Canada), or fluorescent arginine-glycine-aspartic acid (RGD) peptide (CHI Scientific Inc., Maynard, MA) all at a concentration of 25 μg/mL for 5 min under a plasma activated coverslip. The stamps were rinsed with 1× PBS and ddH_2O for 10 s each before rapid drying with a strong pulse of N_2 gas. The inked PDMS stamp was then contacted for 5 s with the desired surface.

Humidified Microcontact Printing (HμCP). Flat PDMS stamps were prepared and inked in the same manner as in μCP. The flat stamps were then quickly rinsed and dried and pressed on a plasma activated patterned stamp for 5 s for dry inking. The patterned stamp was then immediately stamped on the substrate; the hydrophilic channels formed between stamp and substrate were filled with 10 μL of ddH_2O or antibody-supplemented water (100 μg/mL) and incubated for 5 min. After the incubation, the stamp was detached and the substrate rinsed with ddH_2O for 5 s. For the three protein multiprints, the striped stamp was contacted with a clean flat stamp and a second antibody solution flowed through the channels. The flat stamp coated with alternating stripes of two different proteins was contacted with a secondary plasma-activated striped stamp rotated 90° from the direction of the patterned stripes. The two stamps were left in contact for 5 s, and the striped stamp was detached and contacted with the final glass substrate. A third protein solution was filled in the channels and incubated for 5 min before detaching the stamp and rinsing the substrate immediately.

Preparation of Vascularized Stamps. A thin PDMS membrane 100 μm in thickness was fabricated by sandwiching PDMS at a 10:1 ratio between two Teflon-coated glass slides with two layers of Scotch tape on the edges. The PDMS was cured for 24 h before separating the two glass slides and plasma activating the membrane and patterned PDMS striped stamps with 20 μm wide channels and 20 μm stripes. Both components were immediately irreversibly bonded through contact. The bonded stamp was then cut out and extracted in ethanol for 24 h.

HμCP with Vascularized Stamps. Flat PDMS stamps were prepared and inked in the same manner as in μCP. The flat stamps were then quickly rinsed and dried and pressed on a plasma activated patterned stamp for 5 s; the flat stamp with the remaining protein was then immediately stamped on a vascularized stamp for 5 s. The patterned vascularized stamp was then immediately stamped on the substrate, and the channels in the vascularized stamp were filled with 10 μL of a 10% Triton-X100 solution for 5 min. After the incubation, the stamp was detached.

Preparation of Lift-Off Stamps. A computer-generated design of the nanoarrays with 200 nm spots and 1.8 μm spacing was created in Clewin Pro 4.0. A 4 in. silicon wafer was coated with PMMA resist, and the dot arrays were patterned by electron beam lithography (VB6 UHR EWF, Vistec), followed by 100 nm reactive ion etching (System100 ICP380, Plasmalab) into the Si. After cleaning, the wafer was coated with an antiadhesive layer by exposing it to perfluorooctyltriethoxysilane (Sigma-Aldrich, Oakville, ON, Canada) in vapor phase in a desiccator. An accurate polymer copy of the Si wafer was obtained after double replication using poly(dimethylsiloxane) (PDMS) and a UV-sensitive polyurethane.[34] First, an ∼6 mm layer of 1:10 PDMS (Dow Corning, Corning, NY) was poured on the wafer inside a Petri dish, followed by removal of bubbles under vacuum in a desiccator for 10 min. Next, the PDMS was cured in an oven for 24 h at 60 °C (VWR, Montreal, QC, Canada) and then peeled off of the wafer. To remove uncross-linked extractables, the PDMS replica was bathed in 70% ethanol for 24 h and then baked at 60 °C for 4 h. Second, a large drop of UV-sensitive polyurethane (Norland Optical Adhesive 63 (NOA); Norland Products, Cranbury, NJ) was poured on the PDMS and cured by exposing it to 600 W of UV light (Uvitron International, Inc., West Springfield, MA) for 50 s. The PDMS was then peeled off, thus yielding an NOA replica of the Si pattern.

Lift-Off Micro/Nanocontact Printing. A flat PDMS stamp cured against a Si wafer was used for lift-off nanocontact printing against the NOA replicas—now serving as lift-off master—with 200 nm holes. Following removal of the extractables as described above, the flat PDMS stamp was inked for 5 min with a phosphate buffered saline solution (PBS) containing 25 μg/mL of the arginine-glycine-aspartic acid (RGD) peptide (CHI Scientific Inc., Maynard, MA) mixed with 25 μg/mL of chicken immunoglobulin G (IgG) conjugated to Alexa Fluor 488 (Invitrogen, Burlington, ON, Canada) for visualization or

IgG alone for the negative control experiments. After rinsing with PBS and double distilled water for 30 s, the inked stamps were briefly dried under a stream of N_2 and immediately brought into contact with a plasma activated (Plasmaline 415, Tegal, Petaluma, CA) NOA master for 5 s. The PDMS was separated, and the proteins in the contact areas were transferred to the NOA, while the remaining proteins transferred to the final substrate by printing the PDMS stamp for 5 s onto a plasma activated glass coverslip.

Imaging and Analysis. Fluorescently labeled protein micro- and nanopatterns were imaged with fluorescence microscopy (TE2000, Nikon, Saint-Laurent, QC, Canada). Stamp topography was imaged on an inspection microscope (LV150A, Nikon, Saint-Laurent, QC, Canada). Image analysis was performed in ImageJ (NIH, Bethesda, MD). All images were captured with fixed exposure times within each experiment which varied from 1 to 5 s for all the images shown in the article. Image postprocessing to increase the contrast through linear modifications was conducted in ImageJ (NIH, Batesta, MD).

Finite Element Modeling. 2D simulation of molecular diffusion within the PDMS stamp was performed with a finite element model of the fabricated stamps. The water diffusion through the stamp is governed by the general mass balance with negligible convection.[35] The diffusion coefficient of water in PDMS material is reported as 1×10^{-9},[36] 1.2×10^{-9},[37] and 2.49×10^{-9} m^2 s^{-1}.[38] We used 1.2×10^{-9} m^2 s^{-1} for the simulation. The model consists of the cross section of a 1 mm thick structured PDMS stamp with channels formed at the contact between the stamp surface and the substrate. The inner boundaries of the channels were modeled as being saturated with water, while the outer boundaries of the stamp, including sidewalls and the top surface, were void of water. First, the steady state condition of water saturation level in the PDMS was modeled. The concentration of water molecules in PDMS can reach to 40 mol/m^3,[25] while at ambient conditions in air with 100% relative humidity it is only ~1 mol/m^3. In our laboratory, the relative humidity was 40%, corresponding to ~0.4 mol/m^3. For the model, the boundaries at a channel filled with water were fixed as saturated with water (relative concentration $C = 1$) while the boundaries in contact with the environment (sidewalls and top surface) were set to without water ($C = 0$). The water flux at these boundaries was a free parameter. Conversely, at the boundary surface defined as the interface between the stamp and the impermeable glass surface, the concentration was a free parameter while the flux was set to zero. COMSOL Multiphysics 3.5 software (Comsol Inc., Burlington, MA) was used to solve the governing equations based on the above values. First, the steady state solution was calculated, and the water concentration throughout the stamp was expressed in relative concentration C. Second, the time course of water saturation throughout the stamp was solved using the same boundary conditions. The time course of water saturation at the center point of the stripe for different widths is shown in Figure S3.

***Ab Initio* Molecular Models.** A set of SiO_2 with 11 SiO_2 molecules with 33 atoms was optimized to simulate a model of an amorphous glass surface. The string of PDMS consists of 7 units with 72 atoms. For the interaction without water, the interaction between RGD and PDMS was first calculated followed by the addition of SiO_2. For the interaction with water, RGD with water was first calculated and then the entire system including PDMS and SiO_2. The geometry optimization was performed by *ab initio* quantum mechanical calculation of energies using the Gaussian09 package[39] with the standard basis set (mathematical description of the orbitals within a system). The geometry was adjusted until a stationary point on the potential energy surface (PES) was found (that shows the degrees of freedom within the molecule, each point of that surface corresponds to the specific molecular structure—with the height of the surface at that point corresponding to the energy of that structure). The pictures were visualized with the Molden program.[40]

■ ASSOCIATED CONTENT

Supporting Information

Figures S1–S5. This material is available free of charge via the Internet at http://pubs.acs.org.

■ AUTHOR INFORMATION

Corresponding Author

*Fax (+)1 (514) 398 1790; e-mail david.juncker@mcgill.ca (D.J.).

Notes

The authors declare no competing financial interest.

■ ACKNOWLEDGMENTS

We thank Tohid Fatanat Didar for providing fluorescent RGD peptide and BSA for the experiments. We also acknowledge Ali Tamayol, Sébastien Bergeron, and Monika Backhaus for insightful discussions. We acknowledge support from CIHR (Regenerative and Nanomedicine grant), the Canadian Foundation for Innovation and the McGill Nanotools Microfabrication Laboratory (funded by CFI and McGill University). S.G.R. was supported by the CREATE Integrated Sensor System and Neuroengineering program funded both by NSERC and The Molson Foundation. T.E.K. was supported by a Scholarship from the Killam Trust and by a Chercheur Nationaux Award from the Fonds de la Recherche en Santé du Québec. D.J. holds a Canada Research Chair.

■ REFERENCES

(1) Roach, P.; Parker, T.; Gadegaard, N.; Alexander, M. R. Surface strategies for control of neuronal cell adhesion: A review. *Surf. Sci. Rep.* **2010**, *65* (6), 145–173.

(2) Khan, S.; Newaz, G. A comprehensive review of surface modification for neural cell adhesion and patterning. *J. Biomed. Mater. Res., Part A* **2010**, *93A* (3), 1209–1224.

(3) Kim, H. D.; Peyton, S. R. Bio-inspired materials for parsing matrix physicochemical control of cell migration: A Review. *Integr. Biol.* **2012**, *4* (1), 37–52.

(4) Cole, M. A.; Voelcker, N. H.; Thissen, H.; Griesser, H. J. Stimuli-responsive interfaces and systems for the control of protein-surface and cell-surface interactions. *Biomaterials* **2009**, *30* (9), 1827–1850.

(5) Bernard, A.; Delamarche, E.; Schmid, H.; Michel, B.; Bosshard, H. R.; Biebuyck, H. Printing patterns of proteins. *Langmuir* **1998**, *14* (9), 2225–2229.

(6) Renault, J. P.; Bernard, A.; Bietsch, A.; Michel, B.; Bosshard, H. R.; Delamarche, E.; Kreiter, M.; Hecht, B.; Wild, U. P. Fabricating arrays of single protein molecules on glass using microcontact printing. *J. Phys. Chem. B* **2002**, *107* (3), 703–711.

(7) Kaufmann, T.; Ravoo, B. J. Stamps, inks and substrates: polymers in microcontact printing. *Polym. Chem.* **2010**, *1* (4), 371–387.

(8) Tan, J. L.; Tien, J.; Chen, C. S. Microcontact printing of proteins on mixed self-assembled monolayers. *Langmuir* **2002**, *18* (2), 519–523.

(9) Schmalenberg, K. E.; Buettner, H. M.; Uhrich, K. E. Microcontact printing of proteins on oxygen plasma-activated poly(methyl methacrylate). *Biomaterials* **2004**, *25* (10), 1851–1857.

(10) Scholl, M.; Sprossler, C.; Denyer, M.; Krause, M.; Nakajima, K.; Maelicke, A.; Knoll, W.; Offenhausser, A. Ordered networks of rat hippocampal neurons attached to silicon oxide surfaces. *J. Neurosci. Methods* **2000**, *104* (1), 65–75.

(11) Bernard, A.; Renault, J. P.; Michel, B.; Bosshard, H. R.; Delamarche, E. Microcontact printing of proteins. *Adv. Mater.* **2000**, *12* (14), 1067–1070.

(12) Banerjee, I.; Pangule, R. C.; Kane, R. S. Antifouling coatings: Recent developments in the design of surfaces that prevent fouling by proteins, bacteria, and marine organisms. *Adv. Mater.* **2011**, *23* (6), 690–718.

(13) Morra, M.; Occhiello, E.; Marola, R.; Garbassi, F.; Humphrey, P.; Johnson, D. On the aging of oxygen plasma-treated polydimethylsiloxane surfaces. *J. Colloid Interface Sci.* **1990**, *137* (1), 11–24.

(14) Mayer, M.; Yang, J.; Gitlin, I.; Gracias, D. H.; Whitesides, G. M. Micropatterned agarose gels for stamping arrays of proteins and gradients of proteins. *Proteomics* **2004**, *4* (8), 2366−2376.
(15) von Philipsborn, A. C.; Lang, S.; Loeschinger, J.; Bernard, A.; David, C.; Lehnert, D.; Bonhoeffer, F.; Bastmeyer, M. Growth cone navigation in substrate-bound ephrin gradients. *Development* **2006**, *133* (13), 2487−2495.
(16) Hodgkinson, G. N.; Tresco, P. A.; Hlady, V. The differential influence of colocalized and segregated dual protein signals on neurite outgrowth on surfaces. *Biomaterials* **2007**, *28* (16), 2590−2602.
(17) Bernard, A.; Fitzli, D.; Sonderegger, P.; Delamarche, E.; Michel, B.; Bosshard, H. R.; Biebuyck, H. Affinity capture of proteins from solution and their dissociation by contact printing. *Nat. Biotechnol.* **2001**, *19* (9), 866−869.
(18) Didar, T. F.; Foudeh, A. M.; Tabrizian, M. Patterning multiplex protein microarrays in a single microfluidic channel. *Anal. Chem.* **2011**, *84* (2), 1012−1018.
(19) Yoon, J.; Bian, P.; Kim, J.; McCarthy, T. J.; Hayward, R. C. Local switching of chemical patterns through light-triggered unfolding of creased hydrogel surfaces. *Angew. Chem., Int. Ed.* **2012**, *51* (29), 7146−7149.
(20) Coyer, S. R.; Garcia, A. J.; Delamarche, E. Facile preparation of complex protein architectures with sub-100-nm resolution on surfaces. *Angew. Chem., Int. Ed.* **2007**, *46* (36), 6837−6840.
(21) Rodriguez, N. M.; Desai, R. A.; Trappmann, B.; Baker, B. M.; Chen, C. S. Micropatterned multicolor dynamically adhesive substrates to control cell adhesion and multicellular organization. *Langmuir* **2014**, *30* (5), 1327−1335.
(22) Eichinger, C. D.; Hsiao, T. W.; Hlady, V. Multiprotein microcontact printing with micrometer resolution. *Langmuir* **2012**, *28* (4), 2238−2243.
(23) Bharath, R. T.; Michael, E. M.; Jian, G.; Peiming, Z. A nanocontact printing system for sub-100 nm aligned patterning. *Nanotechnology* **2011**, *22* (28), 285302.
(24) Sato, S.; Suzuki, M.; Kanehashi, S.; Nagai, K. Permeability, diffusivity, and solubility of benzene vapor and water vapor in high free volume silicon- or fluorine-containing polymer membranes. *J. Membr. Sci.* **2010**, *360* (1−2), 352−362.
(25) Randall, G. C.; Doyle, P. S. Permeation-driven flow in poly(dimethylsiloxane) microfluidic devices. *Proc. Natl. Acad. Sci. U. S. A.* **2005**, *102* (31), 10813−10818.
(26) Abulencia, J. P.; Theodore, L. *Fluid Flow for the Practicing Chemical Engineer*; John Wiley & Sons: New York, 2011; Vol. *11*.
(27) Mendes, P. M.; Yeung, C. L.; Preece, J. A. Bio-nanopatterning of surfaces. *Nanoscale Res. Lett.* **2007**, *2* (8), 373−84.
(28) Ricoult, S. G.; Pla-Roca, M.; Safavieh, R.; Lopez-Ayon, G. M.; Grutter, P.; Kennedy, T. E.; Juncker, D. Large dynamic range digital nanodot gradients of biomolecules made by low-cost nanocontact printing for cell haptotaxis. *Small* **2013**, *9* (19), 3308−3313.
(29) Lange, S. A.; Benes, V.; Kern, D. P.; Horber, J. K. H.; Bernard, A. Microcontact printing of DNA molecules. *Anal. Chem.* **2004**, *76* (6), 1641−1647.
(30) Weibel, D. B.; Lee, A.; Mayer, M.; Brady, S. F.; Bruzewicz, D.; Yang, J.; DiLuzio, W. R.; Clardy, J.; Whitesides, G. M. Bacterial printing press that regenerates its ink: Contact-printing bacteria using hydrogel stamps. *Langmuir* **2005**, *21* (14), 6436−6442.
(31) Keum, H.; Carlson, A.; Ning, H. L.; Mihi, A.; Eisenhaure, J. D.; Braun, P. V.; Rogers, J. A.; Kim, S. Silicon micro-masonry using elastomeric stamps for three-dimensional microfabrication. *J. Micromech. Microeng.* **2012**, *22* (5).
(32) Lange, S. A.; Benes, V.; Kern, D. P.; Hörber, J. K. H.; Bernard, A. Microcontact printing of DNA molecules. *Anal. Chem.* **2004**, *76* (6), 1641−1647.
(33) Song, J.; Kam, F.-Y.; Png, R.-Q.; Seah, W.-L.; Zhuo, J.-M.; Lim, G.-K.; Ho, P. K.; Chua, L.-L. A general method for transferring graphene onto soft surfaces. *Nat. Nanotechnol* **2013**, *8* (5), 356−362.
(34) Xia, Y. N.; McClelland, J. J.; Gupta, R.; Qin, D.; Zhao, X. M.; Sohn, L. L.; Celotta, R. J.; Whitesides, G. M. Replica molding using polymeric materials: A practical step toward nanomanufacturing. *Adv. Mater.* **1997**, *9* (2), 147−149.
(35) Pedraza, E.; Coronel, M. M.; Fraker, C. A.; Ricordi, C.; Stabler, C. L. Preventing hypoxia-induced cell death in beta cells and islets via hydrolytically activated, oxygen-generating biomaterials. *Proc. Natl. Acad. Sci. U. S. A.* **2012**, *109* (11), 4245−4250.
(36) Leng, J.; Lonetti, B.; Tabeling, P.; Joanicot, M.; Ajdari, A. Microevaporators for kinetic exploration of phase diagrams. *Phys. Rev. Lett.* **2006**, *96* (8).
(37) Watson, J. M.; Payne, P. A. A study of organic-compound pervaporation through silicone-rubber. *J. Membr. Sci.* **1990**, *49* (2), 171−205.
(38) Watson, J. M.; Baron, M. G. The behaviour of water in poly(dimethylsiloxane). *J. Membr. Sci.* **1996**, *110* (1), 47−57.
(39) *Gaussian09*: Frisch, M. J.; Trucks, G. W.; Schlegel, H. B.; Scuseria, G. E.; Robb, M. A.; et al., 2009.
(40) Schaftenaar, G.; Noordik, J. H. Molden: a pre- and post-processing program for molecular and electronic structures. *J. Comput.-Aided Mol. Des.* **2000**, *14* (2), 123−134.